CARBON NANOFIBRES PRODUCED FROM CELLULOSE NANOFIBRES

L. Deng[1*], S. J. Eichhorn[1,2], I. A. Kinloch[1], R. J. Young[1]

[1]*Materials Science Centre, Grosvenor Street, University of Manchester, Manchester, UK, M13 9P*

[2]*College of Engineering, Mathematics and Physical Sciences, University of Exeter, UK, EX4 4AF*

[*]*Email: libo.deng@manchester.ac.uk*

Keywords: Cellulose, carbon nanofibres, Raman spectroscopy

Abstract

Pure cellulose-I nanofibres were fabricated by electrospinning of cellulose acetate (CA) solution followed by deacetylation. These cellulose nanofibres were carbonized using temperatures in the range 400-1500 ºC and the resulting carbon nanofibres (CNFs) were characterized using Raman spectroscopy and transmission electron microscopy (TEM). The crystal size along the basal plane was found to increase with the carbonization temperature and a graphitic structure was observed for fibres treated at a relative low temperature, of 1500 ºC, which suggests the advantage of nano-sized precursors. The modulus of the CNFs, was assessed by an in-situ Raman spectroscopic study of the deformation of CNF/polymer composites, and was found to be ~60 GPa for fibres carbonized at 1500 ºC.

1. Introduction

Carbon fibres are mostly produced from organic precursors such as pitch and poly(acrylonitrile) (PAN). Fibres derived from these precursors have high modulus and strength but are less suitable for heat shielding and ablative applications [1]. Producing carbon fibres from renewable cellulosic precursors has been receiving increasing interest recently. This is due to the abundance and low cost of this precursor, and the comparatively environmentally benign approaches used for fibre production (compared to PAN). The typical sources of cellulose used to make carbon fibres have been primarily viscose and textile-grade rayon fibres. Early studies showed that highly crystalline lyocell fibres might be suitable precursors for carbon fibres, as graphene sheets can develop preferentially along the cellulose crystallites during graphitization [2, 3]. A recent study by our group on Bocell™ fibres-derived carbon fibres showed the resulting fibres (with a diameter of ~6 μm) have a core-shell structure; the shell region had a high modulus, of 140 GPa, and the core region had a modulus of only 40 GPa [4]. The incomplete graphitization found in micron-sized fibres could be overcome using smaller precursor fibres, such as nanofibres, from which a more uniform structure along the radial direction and better mechanical performance is expected.

Electrospinning is a simple yet versatile technique to produce fibres with a diameter ranging from tens of nanometres to a few microns. Direct electrospinning of cellulose solutions involves either a solvent with a high boiling point such as N-methylmorpholine N-oxide (NMMO) or associated salts such as lithium chloride (LiCl) in N, N-dimethylacetamide (DMAc) [5]. Alternatively, cellulose nanofibres can also be produced by firstly

electrospinning of a derivative, such as CA or hydroxypropyl cellulose (HPC), and then regenerating the cellulose. Furthermore, the fibre morphology and diameter, and the porous structure of the fibrous membrane can be readily tuned in the electrospinning process [5].

In the present study, we have successfully produced pure cellulose nanofibres by electrospinning a CA solution in acetone/DMAc, followed by deacetylation in a solution of sodium hydroxide (NaOH) in ethanol. The cellulose nanofibres were then carbonized at temperatures in the range 400 – 1500 ºC, and characterised by Raman spectroscopy and TEM. The modulus of the as-prepared CNFs was also assessed using Raman spectroscopy by following the deformation of a CNF/polymer composite.

2. Experimental

2.1 Materials

CA (average M_n= 100,000 g mol^{-1}), acetone, DMAc, poly(vinyl alcohol) (PVA, M_n= 78000-80000 g mol^{-1}), ethanol and NaOH were purchased from Sigma-Aldrich and used as-received without further purification.

2.2 Electrospinning

The CA was dissolved in a mixed solution of acetone and DMAc (2:1 w:w). Electrospinning was carried out with this solution with a concentration of 20wt%. The spinning conditions were: voltage, 16 kV; flow rate, 0.2 mL h^{-1}; and needle tip-to-collector distance of 16 cm. The fibres were collected using a disk rotating at an angular velocity 1500 rpm to achieve macroscopic alignment for the fibres.

2.3 Deacetylation of CA nanofibres

The electrospun CA fibrous sheets were deacetylated in a 0.05 M NaOH solution in ethanol for 2 days to regenerate into cellulose. The fibrous sheets were then rinsed with water until neutral and kept over ion-exchange resin (Rexyn I-300 H-OH from Fisher Scientific, Inc.) for 7 days to remove the residue metal ions. The samples were thoroughly washed using deionized water and then vacuum-dried at ambient temperature.

2.4 Carbonization of cellulose fibres

The carbonization of the fibres was carried out according to the following procedure.
a) Fibres were initially stabilized by heating to 240 °C in air at a rate of 3 °C min^{-1}, followed by a 60-minute isotherm at the final maximum temperature.
b) The fibres were then carbonized by heating up to 1500 °C in an argon atmosphere at a rate of 10 °C min^{-1}, followed by a 150-minute isotherm at the final maximum temperature.

2.5 Characterisation

Raman spectra were obtained using a Renishaw 1000 system with a He-Ne laser. The morphology of the nanofibres was investigated after gold coating using a Phenom G2 pro desktop SEM, operated at an accelerating voltage of 5 kV. CNFs bundles were sonicated in ethanol for 30 min and deposited onto TEM grids and examined using a Philips CM20 TEM to characterise the microstructures of the CNFs. Thermogravimetric analysis (TGA) and differential scanning calorimetry (DSC) of the regenerated CA nanofibres was carried out using a Jupiter Netzsch STA 449 C instrument. The fibres were placed into an alumina crucible and heated at a rate of 10.0 °C min^{-1}. All thermal analysis was carried out in a nitrogen atmosphere.

2.6 Micromechanical deformation studies using Raman spectroscopy

The CNFs mats were placed on a PMMA beam and covered with a thin layer of PVA. The beam was then inserted into a four-point bending rig and placed onto the Raman microscope stage. Surface strain of the beam during 4-point bending was measured using a resistance strain gauge. The beam was deformed step-wise and Raman spectra were collected from the CNFs at each strain level.

3. Results and discussion

3.1 Morphology and thermal properties of the nanofibres

It was found that electrospinning of CA solutions could be carried out using a broad range of conditions, i.e. with a polymer concentration in the range 10 - 25%, a voltage range of 10 - 25 kV, and tip-to-collector distances of 10 - 25 cm according to our preliminary experiments. The diameter of the fibres spun in these processing windows was found to vary from 0.1 to 1.2 μm, while outside these processing windows, irregular fibres were observed. To achieve macroscopic alignment of the fibres, a rotating disk was employed to collect the fibres during electrospinning. The alignment of the fibres was found to increase with the rotating speed, and good alignment was achieved with an angular velocity of 1500 rpm as shown in Figure 1. The as-spun CA fibres have circular cross-sections with an average diameter of ~450 nm. Upon deacetylation, there was no significant change in the fibre diameter or morphology, but the fibrous sheets were densified.

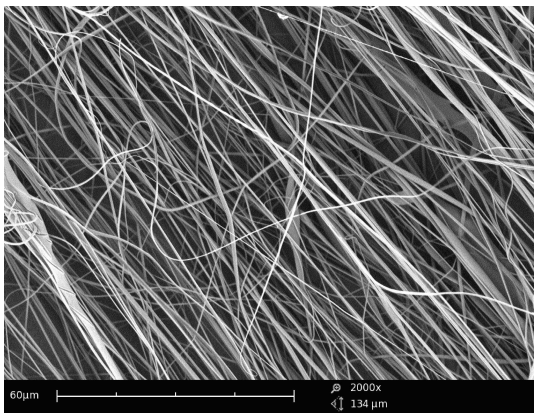

Figure 1. An SEM image of the as-spun CA nanofibres.

Thermal properties of the as-regenerated cellulose and stabilized fibres were investigated using an STA instrument which records the weight loss and heat flow simultaneously. Figure 2a shows the TG curves during the initial pyrolysis process for the as-regenerated cellulose fibres (solid line) in the temperature range 20 - 1000 °C in a nitrogen atmosphere. It can be seen there is a rapid weight loss between 270 and 370 °C, which is due to the degradation of cellulose. Degradation of native and regenerated cellulose has been reported to occur between 200 and 400 ˚C [6, 7], which involves dehydration, thermal cleavage and thermal scission of C=O and C-O bonds. No melting stage is seen from the DSC curve for the as-regenerated cellulose fibres (solid line) as shown in Figure 2b, while a sharp exothermic peak at 290-370 °C is observed, which is related to the stabilization reactions which generate heat in the fibres. TGA performed in air by Tang et al. showed that major pyrolytic degradation begins at 240 °C [7], and hence the stabilization of precursors was carried out at this temperature in the present study. Thermal properties of the precursors stabilized at 240 °C in air for 60 min were then tested under the same conditions and TG and DSC curves are also shown in Figure 2 (dashed lines). It can be seen that after stabilization in air, there is no significant weight loss

between 240 and 400 °C, and no exothermic peak is seen in this case, suggesting that the stabilization reactions have completed and thus our conditions for stabilization are optimal.

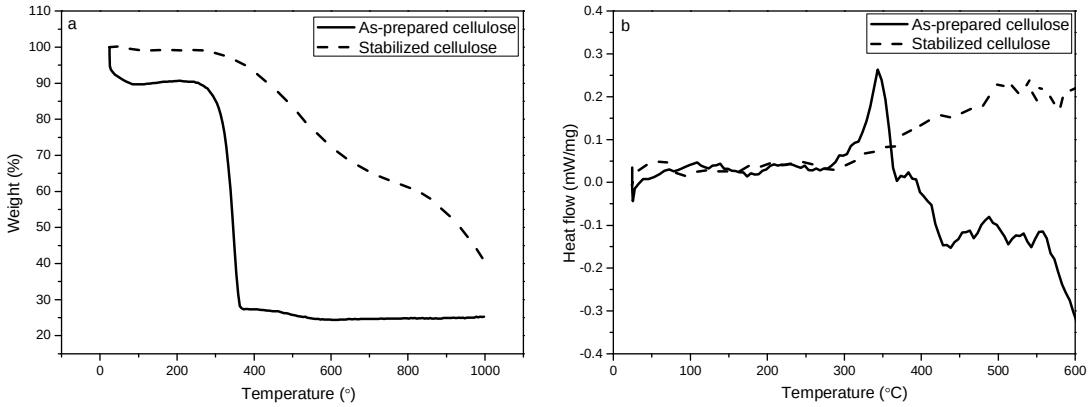

Figure 2. (a) TG and (b) DSC curves for the as-prepared cellulose nanofibres (solid lines) and cellulose nanofibres after stabilized at 240 °C in air for 60 min (dashed lines).

3.2 Carbonization

Cellulose precursors were observed to shrink by ~50% in length during carbonization, with the average diameter decreased from 450 nm to 200 nm, but nevertheless retaining their fibre morphology and macroscopic alignment. TEM images shown in Figure 3a and 3b reveal that the nanofibres treated below 1200 ºC appear to consist of mainly amorphous carbon, while the fibres carbonized at 1500 ºC exhibit turbostratic structure with the graphitic crystallites embedded in an amorphous matrix. The crystallite size along the basal plane in CNFs treated at 1500 ºC is typically ~2 nm. The evolution of crystallite structure is also demonstrated by Raman spectroscopy, as discussed in the following sections.

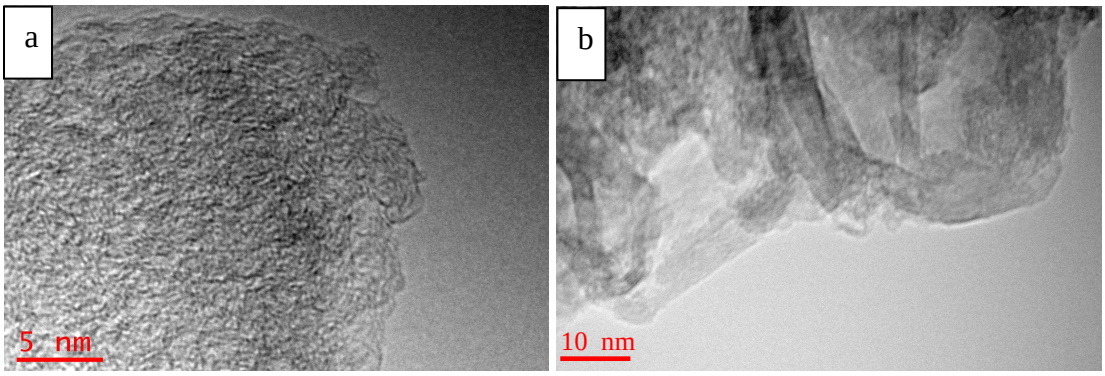

Figure 3. TEM images of CNFs produced by carbonization at 1200 ºC (a) and 1500 ºC (b).

Raman spectroscopy has been used to characterise the CNFs and Figure 4a shows typical Raman spectra of the CNFs carbonized in the temperature range 400 - 1500 ºC. There are two first-order Raman bands that are present in the 1100-1800 cm^{-1} region; namely the D band centred ~1350 cm^{-1} and the G band located at ~1590 cm^{-1}. Generally, the G band is considered to be an in-plane bond stretching motion of sp^2-hybridised C atoms and the D band is related to the breathing mode of the six-fold aromatic ring near the basal edge, although the origin of this band is still debated [8, 9].

Quantitative analysis of Raman spectra relies on accurate determination of spectral parameters which can be obtained by curve fitting. There is, however, no unanimous agreement on the number of peaks, or the correct mathematical functions for fitting Raman spectra in the 1100-1800 cm^{-1} region. Spectra for sp^2-hybridised carbons have been fitted by using two peaks in

many cases [10, 11]; others fitted their spectra using three [12, 13] or five peaks [14, 15]. It is found the spectra for our CNFs are best fitted using three Lorentzian peaks. The extra peak, designated as D″ band and located at ~1500 cm^{-1}, originates from amorphous carbon in the fibres [13, 14]. An example spectrum for CNFs treated at 1000 ºC, with three fitted bands is shown in Figure 4b.

Various spectral indicators, including the intensity ratio between the D and G bands of sp^2 carbons, I_D/I_G, and the bandwidth and frequency of Raman bands have been proposed to characterise different forms of carbonaceous materials in the literature [16]. The I_D/I_G ratio as a function of the carbonization temperature is shown in Figure 4c; a monotonic increase in I_D/I_G with temperature is observed. This behavior is in contrast to that of PAN-based CNFs, where I_D/I_G was found to decreases with the carbonization temperature [11]. The I_D/I_G ratio has been correlated with the in-plane length of graphite crystallites (L_a), firstly by Tuinstra and Koenig [17]. The TK equation, $I_D/I_G = C(\lambda)/L_a$ where $C(\lambda) = 4.4$ nm for a 514 nm laser and L_a was determined by X-ray diffraction, has been widely used to determine the microstructure of various carbonaceous materials. Ferrari and Robertson, however, showed that the TK equation is not valid for small crystallites and they proposed the following relation [8, 9]:

$$I_D / I_G = C'(\lambda) L_a^{\,2} \quad \text{(when } L_a < 2 \text{ nm)} \qquad (1)$$

where $C'(\lambda)$ is a parameter taking into account of the laser effect and has a value of 0.055 for the 514 nm laser. The increase in I_D/I_G with temperature, shown in Figure 4c, suggests that the crystallite size L_a increases with the treatment temperature; these crystallites are small in size, possibly below 2 nm, which is consistent with the TEM observations as shown in Figure 3. It should be noted that Eq. (1) tends to underestimate the crystallite size due to the uncertainty in the origin of the D band [15]. The intensity ratio between the D″ and G bands, $I_{D''}/I_G$, decreases as the temperature increases, as shown in Figure 4c, which suggests a decrease of amorphous carbon fraction with an increasing temperature. Amorphous sp^2 carbons, which give rise to the D″ band, are formed upon thermal scission and cleavage of the glucose rings of cellulose polymers at low temperatures, and are converted to graphitic like layers through aromatization at temperatures higher than 700 ºC [7].

The full width at half maximum (FWHM) of both the D and G bands was found to decrease with an increasing carbonization temperature, as can be seen from Figure 4d. Generally, the broadening of these Raman bands is associated with an increase in disorder. Nakamura *et al.* demonstrated approximately linear relationships between the FWHM of both D and G bands and $1/L_a$ [18]. Yoshida et al. showed the FWHM of the G band is related to the spacing between the graphitic layers, and that the narrowing of the G band indicates a decrease of interlayer spacing and/or transformation from the turbostratic structure to graphitic structure [19]. Therefore, the decrease in FWHM with the temperature for cellulose-based CNFs indicates a higher structural order and crystalline quality at higher temperatures.

It is worth noting that a broad G′ band located at ~2654 cm^{-1} can be seen from the nanofibres carbonized at 1500 ºC, suggesting the presence of graphitic structures in these CNFs. This is in contrast with carbon fibres derived from micron-sized cellulose fibres, where no G′ band was observed at the same carbonization temperature. Graphitisation at a relatively low temperature in these nanofibres suggests the advantage of using nanofibres as precursors for

carbon fibres. The presence of the G′ band also provides an opportunity for investigation of micromechanics in composites, as the position of this band is particularly stress sensitive.

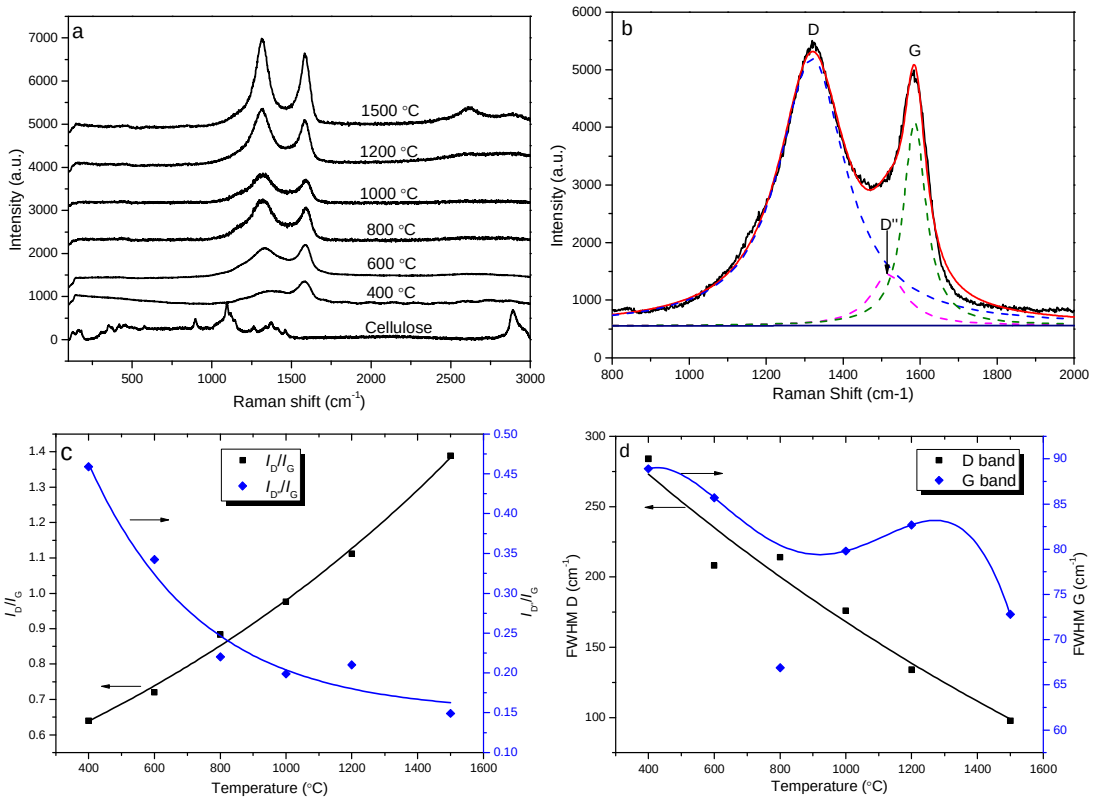

Figure 4. (a) Raman spectra of CNFs treated at different temperatures, (b) an example of curve fitting of a spectrum for CNFs, and (c)-(d) the intensity ratios, I_D/I_G and $I_{D''}/I_G$, and bandwidth as a function of carbonization temperature. Solid lines in (c)-(d) are guides for the eye only.

3.3 Deformation tests

Raman spectroscopy can be used to assess the mechanical properties of CNFs and the interface in a fibre-reinforced composite, based on the fact that Raman bands shift towards a lower wavenumber position under tensile deformation as a result of the elongation of the C-C bonds. The CNFs carbonized at 1500 ºC were embedded in a PVA matrix and deformed using a four-point bending rig. Figure 5 shows the deformation induced shifts in the position of the G′ band, during 4-point bending of the composites. It can be seen that the band position decreases with deformation, in the low strain range, and a maximum shift is observed at ~0.4% strain, after which no obvious downshift was observed due possibly to the breakdown of the interface in the composite. The Raman band shift rate with respect to strain was obtained by fitting the data linearly in the strain range 0 - 0.4%; this value was found to be -3 cm^{-1}/%. Cooper *et al.* investigated the deformation of a number of different carbon fibres and showed that the G′ band shift rate with respect to strain is proportional to the carbon fibre modulus [20]. They went on to suggest that there is a universal calibration of -5 $cm^{-1}\%^{-1}$/GPa for the stress-induced shifts of the G′ band. This calibration has been extensively used to estimate the modulus of carbon nanotubes and graphene [21]. Assuming that the calibration is also valid for the shift of the same G′ band in our CNFs, a shift rate of -3 cm^{-1}/% suggests a modulus of ~60 GPa for the CNFs. Our recent work on carbon fibres produced by pyrolysis of highly crystalline cellulose fibre at 2500 ºC exhibited a modulus of 140 GPa for the skin and 40 GPa for the core region [4]. It has been reported in the literature that rayon-based carbon

fibres have a modulus of typically 40-100 GPa, and lyocell-based carbon fibres a modulus of 90-100 GPa [2]. It should be noted that the pyrolysis in Ref. [2] was carried out in the presence of NH_4Cl which is well-known as a catalyst that promotes the stabilization and graphitization of cellulose, and also protect the fibre surface [22]. No catalyst was used in the present work, which could be one reason for the difference. Our most recent work has also shown that graphitization of cellulose nanofibres, aided by nucleating agents, leads to an even higher modulus for the CNFs.

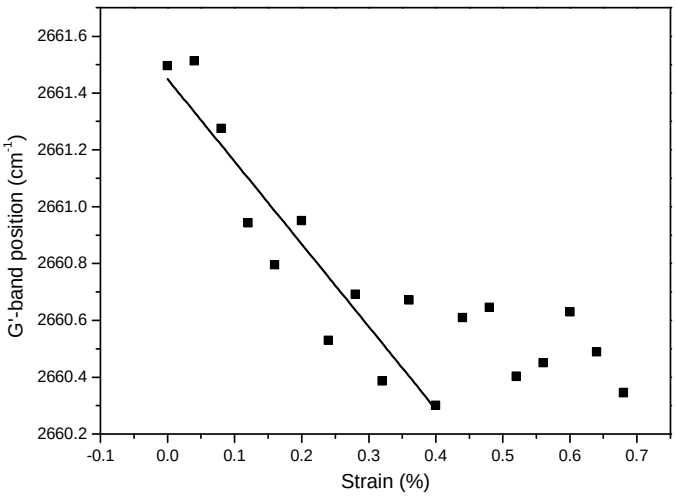

Figure 5. The G′ Raman peak position as a function of strain for a CNF/PVA composite.

4. Conclusions

Cellulose-I nanofibres were fabricated by electrospinning of CA solution in acetone/DMAc followed by deacetylation to regenerate to cellulose fibres. The cellulose fibres were carbonized over a temperature range 400-1500 ºC and the resulting carbon nanofibres were characterised using Raman spectroscopy and TEM. The crystal size along the basal plane was found to increase with the carbonization temperature, but was smaller than 2 nm for all CNFs. Graphitic structure was observed for fibres treated at a relatively low temperature. The modulus of the CNFs, assessed by in-situ Raman spectroscopic study of the deformation of CNF/polymer composites, was found to be ~60 GPa, thus showing the advantage of using cellulose nanofibres as precursors.

References

1. Dumanh, A.G. and A.H. Windle, Carbon fibres from cellulosic precursors: a review, *J. Mater. Sci.* **47**: p. 4236-4250 (2012).
2. Peng, S., H. Shao, and X. Hu, Lyocell fibers as the precursor of carbon fibers, *J. Appl. Polym. Sci.* **90**: p. 1941-1947 (2003).
3. Zhang, H., L. Guo, H. Shao, and X. Hu, Nano-carbon black filled Lyocell fiber as a precursor for carbon fiber, *J. Appl. Polym. Sci.* **99**: p. 65-74 (2006).
4. Kong, K., L. Deng, I.A. Kinloch, R.J. Young, and S.J. Eichhorn, Production of carbon fibres from a pyrolysed and graphitised liquid crystalline cellulose fibre precursor, *J. Mater. Sci*. **47**: p. In press (2012).
5. Lu, P. and Y.L. Hsieh, Multiwalled carbon nanotubes (MWCNT) reinforced cellulose fibres by electrospinning, *ACS Appl. Mater. Interfaces*. **2**: p. 2413-2420 (2010).
6. Plaisantin, H., R. Pailler, A. Guette, G. Daude, M. Petraud, B. Barbe, M. Birot, J.P. Pillot, and P. Olry, Conversion of cellulosic fibres into carbon fibres: a study of the mechanical

properties and correlation with chemical structure *Comp. Sci. Technol.* **61**: p. 2063-2068 (2001).
7. Tang, M.M. and R. Bacon, Carbonization of cellulose fibres-1 Low temperature pyrolysis, *Carbon*. **2**: p. 211-220 (1964).
8. Ferrari, A.C. and J. Robertson, Interpretation of Raman spectra of disordered and amorphous carbon, *Phys. Rev. B.* **61**: p. 14095 1-13 (2000).
9. Ferrari, A.C. and J. Robertson, Resonant Raman spectroscopy of disordered, amorphous, and diamondlike carbon, *Phys. Rev. B.* **64**: p. 075414 1-13 (2001).
10. Paris, O., C. Zollfrank, and G.A. Zickler, Decomposition and carbonisation of wood biopolymers - a microstructural study of softwood pyrolysis *Carbon*. **43**: p. 53-66 (2005).
11. Wang, Y., S. Serrano, and J.J. Santiago-Aviles, Raman characterization of carbon nanofibers prepared using electrospinning, *Synthetic Met.* **138**: p. 423-427 (2003).
12. Kim, C., S.H. Park, J.I. Cho, D.Y. Lee, T.J. Park, W.K. Lee, and K.S. Yang, Raman spectroscopic evaluation of polyacrylonitrile-based carbon nanofibers prepared by electrospinning *J. Raman Spectrosc.* **35**: p. 928-933 (2004).
13. Xue, P., J. Gao, Y. Bao, J. Wang, Q. Li, and C. Wu, An analysis of microstructural variations in carbon black modified by oxidation or ultrasound, *Carbon*. **49**: p. 3346-3355 (2011).
14. Sadezky, A., H. Muckenhuber, H. Grothe, R. Niessner, and U. Pöschl, Raman microspectroscopy of soot and related carbonaceous materials: Spectral analysis and structural information, *Carbon*. **43**: p. 1731-1742 (2005).
15. Zickler, G.A., B. Smarsly, N. Gierlinger, H. Peterlik, and O. Paris, A reconsideration of the relationship between the crystallite size L-a of carbons determined by X-ray diffraction and Raman spectroscopy *Carbon*. **44**: p. 3239-3246 (2006).
16. Larouche, N. and B.L. Stansfield, Classifying nanostructured carbons using graphitic indices derived from Raman spectra, *Carbon*. **48**: p. 620-629 (2010).
17. Tuinstra, F. and J.L. Koenig, Raman spectrum of graphite, *J. Chem. Phys.* . **53**: p. 1126-1130 (1970).
18. Nakamura, K., M. Fujitsuka, and M. Kitajima, Disorder-induced line broadening in 1st-order Raman scattering from graphite, *Phys. Rev. B.* **41**: p. 12260-12263 (1990).
19. Yoshida, A., Y. Kaburagi, and Y. Hishiyama, Full width at half maximum intensity of the G band in the first order Raman spectrum of carbon material as a parameter for graphitization *Carbon*. **44**: p. 2333-2335 (2006).
20. Cooper, C., R. Young, and M. Halsall, Investigation into the deformation of carbon nanotubes and their composites through the use of Raman spectroscopy, *Compos. Part A.* **32**(3-4): p. 401-411 (2001).
21. Deng, L., S.J. Eichhorn, C.C. Kao, and R.J. Young, The Effective Young's Modulus of Carbon Nanotubes in Composites, *ACS Appl. Mater. Interfaces*. **3**: p. 433-440 (2011).
22. Li, H., Y. Yang, Y. Wen, and L. Liu, A mechanism study on preparation of rayon based carbon fibers with (NH4)2SO(4)-NH4Cl-organosilicon composite catalyst system, *Comp. Sci. Technol.* **67**: p. 2675-2682 (2007).